Structural characterisation and sorption capability of whey protein aerogels obtained by freeze-drying or supercritical drying

Food Hydrocolloids

Structural characterization and sorption capability of w hey protein aerogels obtained by freeze-drying or supercritical drying

--Manuscript Draft--

Manuscript Number:	
Article Type:	Research paper
Keywords:	whey protein isolate; freeze-drying; supercritical-CO2-drying; microstructure, absorption, delivery systems
Corresponding Author:	Stella Plazzotta Department of Agricultural, Food, Environmental and Animal Sciences, University of Udine Udine, Udine Italy
First Author:	Lara Manzocco
Order of Authors:	Lara Manzocco
	Stella Plazzotta
	Jeffery Powell
	Auke de Vries
	Dérick Rousseau
	Sonia Calligaris
Abstract:	Whey protein isolate (WPI) hydrogels were converted into aerogels by freeze-drying (FD) or supercritical drying (SCD). SCD resulted in denser aerogels, with a network of closely-associated WPI microgel aggregates, and pore size < 1 μm in diameter. In the FD aerogels, individual aggregates were fused and formed a self-supporting protein matrix with larger pores (2-5 μm in diameter). Both aerogels showed a glass transition at 161 ± 4 °C and maintained their original porosity at room temperature at an equilibrium relative humidity < 80 %. The kinetics of both water and oil uptake were slower in the SCD aerogel than in the FD aerogel. While water absorption caused aerogel swelling and destructuring, the oil-loaded aerogels retained their integrity and adsorbed up to 75 % (w/w) oil. The oil-loaded aerogels showed differences in firmness and oil holding capacity (OHC) depending on the drying procedure applied: SCD samples presented a higher firmness (~ 30 N) and OHC (~ 96 %) than the FD samples (~ 19 N, OHC ~ 45 %). This study demonstrates that the drying technique used can substantially alter the functional attributes of whey protein aerogels.
Suggested Reviewers:	Isabella Jung Hamburg University of Technology: Technische Universitat Hamburg isabella.jung@tuhh.de Expert in development and characterization of bioaerogels
	David Andlinger Technical University of Munich: Technische Universitat Munchen david.andlinger@tum.de Expert in development and characterization of protein bioaerogels
	Alejandro Marangoni University of Guelph amarango@uoguelph.ca Expert in physical properties of foods and food ingredients
	Carlos Garcia Gonzalez Universidad de Santiago de Compostela: Universidade de Santiago de Compostela carlos.garcia@usc.es Expert in development and characterization of bioaerogels

Dear Editor,

We send to your attention the research article " **Structural characterization and sorption capability of whey protein aerogels obtained by freeze-drying or supercritical drying**" by Lara Manzocco, Stella Plazzotta, Jeffery Powell, Auke de Vries, Dérick Rousseau, and Sonia Calligaris.

All authors concur with the submission. Following, we report the Abstract:

Whey protein isolate (WPI) hydrogels were converted into aerogels by freeze-drying (FD) or supercritical drying (SCD). SCD resulted in denser aerogels, with a network of closely-associated WPI microgel aggregates, and pore size < 1 μm in diameter. In the FD aerogels, individual aggregates were fused and formed a self-supporting protein matrix with larger pores (2-5 μm in diameter). Both aerogels showed a glass transition at 161 ± 4 °C and maintained their original porosity at room temperature at an equilibrium relative humidity < 80 %. The kinetics of both water and oil uptake were slower in the SCD aerogel than in the FD aerogel. While water absorption caused aerogel swelling and destructuring, the oil-loaded aerogels retained their integrity and adsorbed up to 75 % (w/w) oil. The oil-loaded aerogels showed differences in firmness and oil holding capacity (OHC) depending on the drying procedure applied: SCD samples presented a higher firmness (~ 30 N) and OHC (~ 96 %) than the FD samples (~ 19 N, OHC ~ 45 %). This study demonstrates that the drying technique used can substantially alter the functional attributes of whey protein aerogels.

The authors believe that the current research article is perfectly in line with the topics covered by the Food Hydrocolloids. We hope that this article could satisfy the requirements of this Journal, so that you might consider it for publication.

Best regards,

Stella Plazzotta, PhD
Section of Food Chemistry and Technology
Department of Agricultural, Food, Environmental and Animal Sciences, University of Udine
Via Sondrio 2/A
33100 Udine, Italy
stella.plazzotta@uniud.it

Highlights

- Whey protein microgels can be converted into aerogels
- Aerogel porosity lower with supercritical drying versus freeze-drying
- Aerogels undergo destructuring upon water absorption
- Oil-loaded aerogels hold up to 75% of their mass as oil
- Aerogel firmness and oil retention higher with supercritical drying

Graphical Abstract

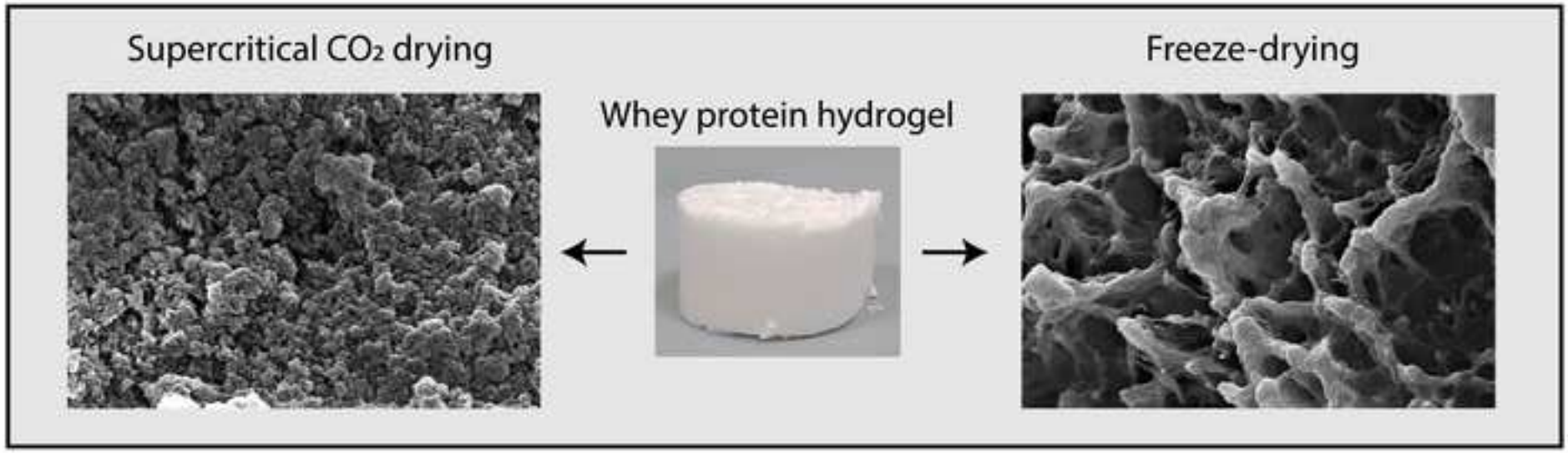

Structural characterization and sorption capability of whey protein aerogels obtained by freeze-drying or supercritical drying

Lara Manzocco[1], Stella Plazzotta[1*], Jeffery Powell[2], Auke de Vries[2], Dérick Rousseau[2], Sonia Calligaris[1]

[1] Department of Agricultural, Food, Environmental and Animal Sciences, University of Udine, Via Sondrio 2/A, 33100 Udine, Italy

[2] Department of Chemistry and Biology, Ryerson University, 350 Victoria St., Toronto, Ontario, Canada M5B 2K3

[*]Corresponding author

e-mail: stella.plazzotta@uniud.it

Abstract

Whey protein isolate (WPI) hydrogels were converted into aerogels by freeze-drying (FD) or supercritical drying (SCD). SCD resulted in denser aerogels, with a network of closely-associated WPI microgel aggregates, and pore size < 1 μm in diameter. In the FD aerogels, individual aggregates were fused and formed a self-supporting protein matrix with larger pores (2-5 μm in diameter). Both aerogels showed a glass transition at 161 ± 4 °C and maintained their original porosity at room temperature at an equilibrium relative humidity < 80 %. The kinetics of both water and oil uptake were slower in the SCD aerogel than in the FD aerogel. While water absorption caused aerogel swelling and destructuring, the oil-loaded aerogels retained their integrity and adsorbed up to 75 % (w/w) oil. The oil-loaded aerogels showed differences in firmness and oil holding capacity (OHC) depending on the drying procedure applied: SCD samples presented a higher firmness (~ 30 N) and OHC (~ 96 %) than the FD samples (~ 19 N, OHC ~ 45 %). This study demonstrates that the drying technique used can substantially alter the functional attributes of whey protein aerogels.

Keywords: whey protein isolate; freeze-drying; supercritical-CO_2-drying; microstructure, absorption, delivery systems

1 Introduction

Aerogels are nanostructured solid materials with low density, open porosity, and high surface area, which are obtained by removing the liquid from a gel. This operation is typically performed by using supercritical carbon dioxide-assisted drying, but freeze-drying is also applied when water is the solvent (Garcia-Gonzalez et al., 2019). These methods generate aerogels with considerably different structures. While supercritical CO_2 drying generally allows for the preservation of polymeric structures by avoiding the formation of liquid-vapour interfaces and presence of capillary tension, freeze-drying commonly results in water expansion upon solidification, often causing macropores and cracks following sublimation (Baudron et al., 2019; Betz et al., 2012; Rodríguez-Dorado et al., 2019). The unique features of aerogels are being explored in many industrial fields, for biomedical, environmental, cosmetic and food applications (www.cost-aerogels.eu; Manzocco et al., 2021). Contrary to other sectors, however, the potential of aerogels in foods remains under-reported.

Protein aerogels have recently attracted attention due to their potential as templates for loading functional ingredients and as delivery systems for human consumption (Ahmadi et al., 2016; Andlinger et al., 2021; Chen et al., 2013; Kleemann et al., 2018, 2020; Plazzotta et al., 2020; Selmer et al., 2015, 2019). For instance, aerogels made of egg-white and dairy proteins have been proposed for the encapsulation and controlled release of fish oil (Ahmadi et al., 2016; Kleemann et al., 2020; Selmer et al., 2019), while whey protein aerogel particles have shown promising results for loading vegetable oils (Plazzotta et al., 2020).

The starting point to prepare protein aerogels is the formation of a hydrogel (Andlinger et al., 2021; Kleemann et al., 2018; Selmer et al., 2015), which is usually obtained by heating a protein solution to induce protein denaturation and form a gel stabilised by disulphide bonds, hydrogen bonding and hydrophobic interactions (Clark et al., 2001; Shimada & Cheftel, 1988). It is known that pH strongly affects the characteristics of the hydrogel and the resulting aerogel (Betz et al., 2012; Clark et al., 2001; Errington & Foegeding, 1998). In the case of whey proteins, a heat treatment near their isoelectric point (5.7) induces the formation of spherical particles ~ 100 nm in diameter. Since these globular structures consist of a hydrated protein network, they are considered microgels (Donato et al., 2011; Nicolai, 2016; Nicolai & Durand, 2013). By increasing the protein concentration, the strands of the microgels randomly associate into larger aggregates, forming self-supporting hydrogels (Nicolai and Durand, 2013), which can then be converted into aerogels by freeze-drying or supercritical CO_2 drying.

Aerogel loading may be easily performed by immersing the aerogel into a target liquid that permeates into the aerogel pores and saturates its internal volume. The liquid retention is generally in the range of 0.2-5.6 g liquid/g aerogel (Kleemann et al., 2020; Plazzotta et al.,

2020; Selmer et al., 2019). Although some aerogels show excellent stability upon liquid uptake (Sharma et al., 2020; Zhang et al., 2016), the immersion liquid may interact with the polymer chains and either reinforce or weaken their architecture. If chain-chain interactions are favoured in the presence of the liquid, significant network contraction can occur along with stiffening of the material (Ahmadi et al., 2016; Manzocco et al., 2017). When the immersion in the liquid disrupts chain-chain interactions in favour of chain-solvent interactions, porosity may decrease and compromise the structural integrity of the aerogel (Antonyuk et al., 2015; Manzocco et al., 2017; Subrahmanyam et al., 2015). Structural integrity upon liquid loading strongly affects the feasibility of exploiting aerogels as delivery systems in foods. In fact, the capability of an aerogel to withstand water or oil environments is a pivotal characteristic not only for the effective entrapment of hydrophilic or lipophilic components, but also for its ability to resist breakdown during food processing, storage and *in vivo* delivery.

In this study, we investigated the potential of whey protein aerogels as delivery materials in foods. Aerogels obtained by freeze-drying (FD) or supercritical drying (SCD) were first characterized for their structural features followed by oil or water loading. The results show the remarkable range of aerogel functional attributes possible depending on the preparation technique applied.

2 Materials and methods

2.1 Whey protein hydrogels

Whey protein gels were made according to the method of Betz et al. (2012). An amount of 20 % (w/w) whey protein isolate (WPI, 94.7 % protein content; 74.6 % β-lactoglobulin, 23.8 % α-lactalbumin, 1.6 % bovine serum albumin, Davisco Food International Inc., Le Sueur, MN, USA) was dissolved in double-distilled water, under continuous stirring at room temperature for 2 h and stored overnight at 4 °C, to ensure complete protein hydration. The pH of the WPI suspension was then adjusted to 5.7 (pH-Meter BASIC 20, Crison, Barcelona, Spain) using a 1 M HCl. Aliquots of 30 mL were then introduced in 50 mL plastic tubes with screwcaps and heated at 85 °C for 30 min using a temperature-controlled water bath to induce protein denaturation. The resulting protein gels were cooled in ice water, stored overnight at 4 °C and cut in cylinders with a height of ~ 1.5 cm and diameter of ~ 2.5 cm.

2.2 Freeze-dried aerogels

Hydrogel cylinders were frozen at −80 °C for 24 h and freeze-dried for 72 h at 4,053 Pa using a pilot plant freeze dryer (Mini Fast 1700, Edwards Alto Vuoto, Milan, Italy). The resulting freeze-dried aerogels were stored in a desiccator containing P_2O_5 at room temperature until use.

2.3 Supercritical-CO_2-dried aerogels

Hydrogel cylinders were converted into alcogels (Manzocco et al., 2017). They were kept at room temperature for 24 hin aqueous solutions of ethanol with increasing concentrations (25, 50, 75 % v/v). Finally, samples were introduced into absolute ethanol twice (for 8 h and then 24 h) to remove residual water before drying using supercritical CO_2. Alcohol removal at 11 ± 1 MPa for 8 hr and 45 °C resulted in the supercritical-CO_2 dried aerogels, which were stored in a desiccator containing P_2O_5 at room temperature until use.

2.4 Aerogel analysis

2.4.1 Image acquisition

Sample images were acquired using an image acquisition cabinet (Immagini & Computer, Bareggio, Italy) equipped with a digital camera (EOS 550D, Canon, Milano, Italy). The camera was placed on an adjustable stand positioned 50 cm above a black cardboard base where the samples were placed. Light was provided by 4 x 100 W frosted photographic floodlights, organized to minimize shadow and glare.

2.4.2 Scanning Electron Microscopy (SEM)

Images of the aerogels were obtained using a ThermoFisher Scientific Quattro S field emission gun environmental scanning electron microscope (SEM) (ThermoFisher, Eindhoven, Netherlands). Samples were prepared for imaging using a Quorum PP3010 Cryo-SEM preparation system (Quorum Technologies, East Sussex, UK). The aerogels were fractured and mounted to aluminium stubs using a carbon tape adhesive (double-sided carbon tape, Electron Microscopy Sciences, Hatfield, Pennsylvania, U.S.A.). The samples were quenched in slushed liquid nitrogen (-220 °C) and inserted into the cryo-preparation chamber. Each sample was sublimated at -90 °C for 5 minutes to remove adsorbed water crystals and then sputter-coated using a Pt target at 5 mA for 60 seconds to reducing electron charging effects. Samples were then transferred to the ESEM chamber and imaged under high vacuum at 140 °C using a secondary electron detector.

2.4.3 Volume and density

Sample volume was calculated as the volume of the cylinder whose diameter and height were measured with CD-15APXR digital calliper (Absolute AOS Digimatic, Mitutoyo Corporation, Kanagawa, Japan). Volume changes following conversion of the hydrogel to an aerogel and following oil absorption were expressed as the percentage ratio between the variation of sample volume to the volume of the corresponding hydrogel. Density was then calculated as the ratio between aerogel weight and sample volume.

2.4.4 Firmness

Firmness was measured by uniaxial compression test using an Instron 4301 (Instron LTD., High Wycombe, UK). The instrumental settings and operation were accomplished using the software

provided by the manufacturer. Samples were tested using a 6.2 mm diameter cylindrical probe mounted on a 1000 N compression head at a 25 mm/min crosshead speed. Force-distance curves were obtained from the compression tests and firmness was taken as the maximum force (N) required to penetrate the sample for 5 mm.

2.4.5 Water vapour sorption

Aerogel samples were weighed and transferred into weighing bottles that were placed in desiccators containing LiCl, CH_3COOK, $MgCl_2$, K_2CO_3, $NaNO_3$, NaCl, KCl, and K_2SO_4 saturated solutions with equilibrium relative humidity (ERH%) values of 11, 25, 32, 43, 65, 75, 86, and 96 %, respectively. Samples were kept inside desiccators until a constant weight was reached. The empirical Freundlich model (Ayawei et al., 2017) (Eq. 1) was used to fit the experimental sorption data.

$$M = k \cdot a_w^{1/n} \quad \text{(Eq. 1)}$$

where M is the equilibrium moisture content on a dry basis (g H_2O/g d.m.), a_w is water activity, k (g H_2O/g d.m.) is the adsorption capacity, and n is a model constant inversely related to extent of adsorption.

2.4.6 Differential Scanning Calorimetry (DSC)

Thermal analysis was carried out using a differential scanning calorimeter (DSC 3 Star^e System, Mettler-Toledo, Greifensee, Swiss) equipped with a Star^e software (ver.16.10, Mettler-Toledo). Heat flow calibration was achieved using indium (heat of fusion 28.45 J/g). Temperature calibration was carried out using hexane (m.p. -93.5 °C), water (m.p. 0.0 °C) and indium (m.p. 156.6 °C). Samples were prepared by carefully weighing ~ 5 mg in 40 µL aluminium DSC pans, which were then hermetically sealed. An empty pan was used as a reference in the DSC cell. Aerogel samples equilibrated at different a_w values were heated from -40 to 150 °C at 10 °C/min. The glass transition temperature (T_g, °C) was determined from the onset temperature of the glass transition of aerogels.

2.4.7 State diagram and modified state diagram

Aerogel state diagrams were obtained by plotting the T_g values for samples equilibrated at different ERH% as a function of the mass fraction of the sample. The obtained curve was fitted using the Gordon-Taylor equation (Eq. 2) (Gordon & Taylor, 1952).

$$T_g = \frac{w_1 T_{g1} + k w_2 T_{g2}}{w_1 + k w_2} \quad \text{(Eq. 2)}$$

where T_{g1} (°C) is the glass transition temperature of the amorphous solute, T_{g2} (°C) is the glass transition temperature of the solvent (-137.5 °C), w_1 and w_2 are the mass fraction of the solute and the solvent, respectively, and k is an experimental constant. The modified state diagram was then obtained by plotting the T_g values for samples equilibrated at different ERH% as a function of their a_w value.

2.4.8 Water and oil absorption kinetics

Aerogel samples were placed into 250 mL beakers filled with 125 mL of water or sunflower oil at room temperature (22 °C). At defined time intervals, samples were withdrawn, the surface was carefully blotted dry with absorbent paper, and weighed until a constant weight in three consecutive measurements was reached. Absorbed water or oil was expressed as the ratio between weight gain at time t (min) to the initial weight of the aerogel sample.

2.4.9 Oil content

The oil content of the samples was defined as the % ratio between the amount of oil at the absorption plateau value and the sample weight.

2.4.10 Oil holding capacity

Around 100-200 mg of sample was placed into 1.5 mL microtubes between two pieces of absorbing paper. Samples were centrifuged at 13,000 rpm (15,871 x g) for 30 min using a microcentrifuge (Mikro 120, Hettich Zentrifugen, Andreas Hettich GmbH and Co, Tuttlingen, Germany). Oil holding capacity (OHC) was computed as the % ratio between the weight of oil retained in the aerogel after centrifugation and the total weight of oil in the sample before centrifugation.

2.5 Data analysis

Data were expressed as the mean ± standard error (SE) of at least two measurements from two experimental replicates ($n \geq 4$). Statistical analysis was performed by using R v. 3.0.2 (The R Foundation for Statistical Computing). Student's t-test was used to determine statistically significant differences between means ($p < 0.05$). Non-linear regression analysis of M values as a function of aerogel a_w and of T_g values as a function of aerogel mass fraction was performed by using TableCurve2D software (Jandel Scientific, ver. 5.01). The goodness of fit was evaluated based on statistical parameters of fitting (R^2).

3 Results and discussion

Figure 1 shows the visual appearance and microstructure of whey protein aerogels obtained by freeze-drying (FD) or supercritical CO_2-drying (SCD). In agreement with the findings of Betz et al. (2012), both aerogels appeared visually opaque. FD aerogels showed an uneven surface with evident cracking. The SCD aerogel appeared more homogeneous without large cracks or crevices.

Important morphological differences between the samples were observed via SEM. The microstructure of the FD samples (Figures 1B and 1C) suggested an open protein matrix consisting of large pores, in agreement with other studies (Betz et al., 2012; Jin et al., 2004; Nazarov et al., 2004). This morphology may have resulted from ice crystal formation during hydrogel freezing, which forced the whey protein microgels to freeze-concentrate. When these ice crystals are sublimated during FD, liquid-vapour interfaces and capillary surface tension are avoided (Fricke & Tillotson, 1997). It is likely that the protein network structure was altered during the freezing phase, with limited effect of the subsequent sublimation of ice crystals. The structural rearrangement resulted in larger pores and a larger void volume.

A compact and homogeneous matrix was observed in SCD samples at low magnification (Figure 1E). At higher magnification (Figure 1F), we observed the presence of a particulate network of interconnected spherical aggregates, similar to whey protein microgels in aqueous environments (Donato et al., 2011; Nguyen et al., 2016). This suggested that supercritical drying preserved the structure and organisation of the original microgel particles. The result of this assembly was a 3D network with pores in the low-micron range and a smaller void volume.

Table 1 highlights key aerogel properties. Conversion of the hydrogels into aerogels resulted in volume shrinkage, which was significantly greater for the SCD aerogels (~ 39 %) compared to the FD aerogels (~ 15 %). Accordingly, the FD aerogels were significantly softer than SCD samples and also presented a 25 % lower density (Table 1). It is likely that in the SCD aerogels, the polarity of the environment surrounding whey protein microgel progressively decreased due to water substitution by ethanol, and ethanol removal by CO_2. Such a change in polarity likely weakened the interactions between the proteins and solvent and favoured those among whey proteins chains, resulting in contraction of the gel (Ganesan et al., 2018). However, the original particulate microstructure would not be lost, providing the architecture observed by SEM (Figure 1).

Table 1. Volume contraction, firmness, density, and experimental regression coefficient estimates *k* and *n* for the Freundlich model (Eq .1) of aerogels obtained by freeze-drying (FD) and supercritical-CO_2-drying (SCD).

Drying technique	Volume contraction (%)*	Firmness (N)	Density (g/cm^3)	*k* (g H_2O/g d.m.)	*n*
FD	-14.67 ± 5.08 [a]	15.9 ± 0.2 [b]	0.22 ± 0.01[a]	0.312 ± 0.012	0.401 ± 0.031
SCD	-38.64 ± 3.86 [b]	47.5 ± 0.3 [a]	0.29 ± 0.02 [b]	0.603 ± 0.047	0.148 ± 0.020

[a,b]: Means in the same column indicated by different letters are statistically different ($p < 0.05$)

* Volume contraction is expressed in relation to original hydrogel

To better understand the capacity of aerogels to interact with water vapour, aerogels were equilibrated at increasing relative humidity. Figure 2 shows aerogel moisture adsorption as a function of a_w. The increase in the relative water vapour pressure was associated with a limited but progressive increase in moisture. Such behaviour can be described by type III isotherms, indicating that both samples had a limited capacity of interacting with water molecules. Water would be mostly adsorbed due to interactions with previously adsorbed water layers rather than with the aerogel surface. Such isotherms are typically modelled with the Freundlich model (De Smedt et al., 2015) which, here, closely fitted the experimental data ($R^2 > 0.97$) with significant parameter estimates ($p < 0.001$). Although the model parameters for the two aerogels resulted in the same order of magnitude, the adsorption capacity (*k*) was higher in the SCD vs. the FD aerogels whereas the adsorption intensity (*n*) was greater in the FD than in the SCD aerogels (Table 1). Over the a_w range, the FD aerogels showed a higher adsorption ability at a_w values below 0.80, while above this value, the SCD samples showed a higher adsorption capacity. Such differences were likely to be due to the different surface areas of the two samples (Figure 1). The limited ability of the aerogels to interact with water vapour was probably due to the changes in protein conformation upon heat-induced gelation. According to Iglesias, Chirife, and Lombardi (1975), the formation of hydrogen bonds among whey proteins might reduce their availability for surface interaction between proteins and water. The availability of surface hydrogen groups would be further decreased by the engagement of protein functional groups in protein-protein interactions, which are the basis for self-supporting aerogels.

The drying technique did not affect the thermal stability of the dried aerogels. Both types of aerogels underwent a glass transition at 161 ± 4 °C (Figure 3). Glass transition temperature data were modelled as a function of mass fraction using the Gordon-Taylor equation (Gordon & Taylor, 1952). Non-linear regression analysis showed good determination coefficients (≥ 0.97) and significant ($p < 0.001$) values of the model experimental constant (*k*). No significant

differences in *k* values ($p \geq 0.05$) between the FD and SCD aerogels were detected. This showed that the physical stability of the aerogels at different relative humidity values was mainly controlled by the intrinsic properties of the whey proteins rather than by their porosity. A similar effect was previously observed in aerogels made with κ-carrageenan (Manzocco et al., 2017), which presented considerably different microstructures but comparable isotherms and glass transitions. Figure 3 also shows that at 20 °C, both aerogels were in the glassy state and turned to a rubbery state when they adsorbed an amount of water equal to ~ 20 % of the aerogel sample mass. Whey protein aerogels would thus remain physically stable and maintain their original porosity at room temperature if kept at ERH lower than ~ 80 %. Based on these considerations, the present whey protein aerogels may be regarded as materials easy to store and manage, thereby providing an advantage for use as food ingredients.

The loading potential of the aerogels was investigated by immersing them in water or oil (Figure 4). Water absorption by aerogels was associated with swelling and loss of the original shape of the samples (Figure 4A). Although both samples swelled, the FD aerogel showed faster water uptake, given its higher porosity (Figure 1) and water vapour adsorption (Figure 2).

Oil absorption by the FD aerogels occurred in less than 1 minute, but was more gradual in the SCD aerogel, levelling off after 100 minutes (Figure 4B). Despite these differences, the final oil uptake was ~ 75 % for both aerogels (Table 2). There was no obvious link between oil loading and aerogel swelling or surface solubilisation (Figure 4B). However, a remarkable contraction in sample volume was observed in the SCD aerogel, suggesting that its protein network further shrunk upon oil absorption (Table 2). Oil entrapment also significantly decreased aerogel firmness (Tables 1 and 2, $p < 0.05$), indicating that the presence of oil weakened the protein network, similar to the water absorption results. By contrast, there was near instantaneous and sponge-like absorption of oil in the FD aerogel, which was accompanied by minimal volume contraction (- 7 % as compared to the starting aerogel) and firmness values similar to the unloaded aerogel (Table 1). The dissimilar oil adsorption kinetics likely resulted from the different pore sizes present in the aerogels (Figure 1), and were consistent with smaller void fractions resulting in a higher plateau adsorption value being reached at a slower rate compared to a material with a larger void volume (Khosravi & Azizian, 2016).

Table 2. Volume contraction, firmness, oil content and oil holding capacity (OHC) of oil-loaded aerogels obtained by freeze-drying (FD) and supercritical-CO_2-drying (SCD).

Drying technique	Volume contraction (%)*	Firmness (N)	Oil content (%)	OHC (%)
FD	-21.46 ± 0.90 [a]	18.5 ± 0.2 [a]	73.5 ± 0.1 [a]	44.7 ± 0.9 [a]
SCD	-54.14 ± 0.29 [b]	29.5 ± 0.2 [b]	76.5 ± 0.6 [a]	96.3 ± 0.9 [b]

[a,b]: In the same column, means indicated by different letters are statistically different ($p < 0.05$)

* Volume contraction is expressed in relation to original hydrogel

Conclusions

The morphology and porosity of aerogels obtained by freeze-drying or supercritical drying were remarkably different. The former resulted in aerogels with larger pores and a greater void volume compared to the latter. Such differences suggested that it would be possible to modify the material performance towards a target application by choosing a different drying technique. If fast dissolution of an aerogel upon contact with water is the targeted application, freeze-dried aerogels should be selected. By contrast, when oil is to be tightly retained within the protein network structure, the use of supercritical dried protein aerogels could be an option.

Given their ability to absorb oil, future studies will examine the potential of whey protein aerogels as transport matrices for labile, oil-soluble compounds. Such studies will determine how aerogels may protect ingredients during shelf life studies and during passage within the digestive tract. This approach will be used to maximize their performance both in food products and, eventually, *in-vivo*.

Funding

Work carried out in the framework of COST Action CA18125 “Advanced Engineering and Research of aeroGels for Environment and Life Sciences” (AERoGELS), funded by the European Commission". Funding from the Natural Sciences and Engineering Research Council of Canada is acknowledged.

Declaration of Competing Interest

The authors declare that they have no known competing financial interests or personal relationships that could have appeared to influence the work reported in this paper.

References

Ahmadi, M., Madadlou, A., Akbar, A., & Saboury, A. A. (2016). Whey protein aerogel as

blended with cellulose crystalline particles or loaded with fish oil. *Food Chemistry*, *196*, 1016–1022. https://doi.org/10.1016/j.foodchem.2015.10.031

Andlinger, D. J., Bornkeßel, A. C., Jung, I., Schroeter, B., Smirnova, I., & Kulozik, U. (2021). Microstructures of potato protein hydrogels and aerogels produced by thermal crosslinking and supercritical drying. *Food Hydrocolloids*, *112*, 106305. https://doi.org/https://doi.org/10.1016/j.foodhyd.2020.106305

Antonyuk, S., Heinrich, S., Gurikov, P., Raman, S., & Smirnova, I. (2015). Influence of coating and wetting on the mechanical behaviour of highly porous cylindrical aerogel particles. *Powder Technology*, *285*, 34–43. https://doi.org/https://doi.org/10.1016/j.powtec.2015.05.004

Ayawei, N., Ebelegi, N., & Wankasi, D. (2017). *Modelling and Interpretation of Adsorption Isotherms*. https://doi.org/10.1155/2017/3039817

Baudron, V., Gurikov, P., Smirnova, I., & Whitehouse, S. (2019). Porous starch materials via supercritical-and freeze-drying. *Gels*, *5*, 9–13. https://doi.org/10.3390/gels5010012

Betz, M., García-González, C. A., Subrahmanyam, R. P., Smirnova, I., & Kulozik, U. (2012). Preparation of novel whey protein-based aerogels as drug carriers for life science applications. *Journal of Supercritical Fluids*, *72*, 111–119. https://doi.org/10.1016/j.supflu.2012.08.019

Chen, H. B. B., Wang, Y. Z. Z., & Schiraldi, D. A. (2013). Foam-like materials based on whey protein isolate. *European Polymer Journal*, *49*, 3387–3391. https://doi.org/10.1016/j.eurpolymj.2013.07.019

Clark, A. H., Kavanagh, G. M., & Ross-Murphy, S. B. (2001). Globular protein gelation-Theory and experiment. *Food Hydrocolloids*, *15*, 383–400. https://doi.org/10.1016/S0268-005X(01)00042-X

De Smedt, C., Ferrer, F., Leus, K., & Spanoghe, P. (2015). Removal of pesticides from aqueous solutions by adsorption on zeolites as solid adsorbents. *Adsorption Science and Technology*, *33*, 457–485. https://doi.org/10.1260/0263-6174.33.5.457

Donato, L., Kolodziejcyk, E., & Rouvet, M. (2011). Mixtures of whey protein microgels and soluble aggregates as building blocks to control rheology and structure of acid induced cold-set gels. *Food Hydrocolloids*, *25*, 734–742. https://doi.org/10.1016/j.foodhyd.2010.08.020

Errington, A. D., & Foegeding, E. A. (1998). Factors determining fracture stress and strain of fine-stranded whey protein gels. *Journal of Agricultural and Food Chemistry*, *46*, 2963–2967. https://doi.org/10.1021/jf980112y

Fricke, J. U., & Tillotson, T. (1997). Aerogels: production, characterization, and applications.

Thin Solid Films, *297*, 212–223. https://doi.org/10.1016/S0040-6090(96)09441-2

Ganesan, K., Budtova, T., Ratke, L., Gurikov, P., Baudron, V., Preibisch, I., Niemeyer, P., Smirnova, I., & Milow, B. (2018). Review on the production of polysaccharide aerogel particles. *Materials*, *11*, 1–37. https://doi.org/10.3390/ma11112144

Garcia-Gonzalez, C. A., Budtova, T., Durães, L., Erkey, C., Del Gaudio, P., Gurikov, P., Koebel, M., Liebner, F., Neagu, M., & Smirnova, I. (2019). An opinion paper on aerogels for biomedical and environmental applications. *Molecules*, *24*, 1815.

Gordon, M., & Taylor, J. S. (1952). Ideal copolymers and the second-order transitions of synthetic rubbers. i. non-crystalline copolymers. *Journal of Applied Chemistry*, *2*, 493–500. https://doi.org/https://doi.org/10.1002/jctb.5010020901

Iglesias, H. A., Chirife, J., & Lombardi, J. L. (1975). Comparison of water vapour sorption by sugar beet root components. *International Journal of Food Science & Technology*, *10*, 385–391. https://doi.org/https://doi.org/10.1111/j.1365-2621.1975.tb00044.x

Jin, H., Nishiyama, Y., Wada, M., & Kuga, S. (2004). Nanofibrillar cellulose aerogels. *Colloids and Surfaces A: Physicochemical and Engineering Aspects*, *240*, 63–67. https://doi.org/10.1016/j.colsurfa.2004.03.007

Khosravi, M., & Azizian, S. (2016). A new kinetic model for absorption of oil spill by porous materials. *Microporous and Mesoporous Materials*, *230*, 25–29. https://doi.org/10.1016/j.micromeso.2016.04.039

Kleemann, C., Schuster, R., Rosenecker, E., Selmer, I., Smirnova, I., & Kulozik, U. (2020). In-vitro-digestion and swelling kinetics of whey protein, egg white protein and sodium caseinate aerogels. *Food Hydrocolloids*, *101*, 105534. https://doi.org/10.1016/j.foodhyd.2019.105534

Kleemann, C., Selmer, I., Smirnova, I., & Kulozik, U. (2018). Tailor made protein based aerogel particles from egg white protein, whey protein isolate and sodium caseinate: Influence of the preceding hydrogel characteristics. *Food Hydrocolloids*, *83*, 365–374. https://doi.org/10.1016/j.foodhyd.2018.05.021

Manzocco, L., Mikkonen, K. S., & García-González, C. A. (2021). Aerogels as porous structures for food applications: Smart ingredients and novel packaging materials. *Food Structure*, *28*, 100188. https://doi.org/10.1016/j.foostr.2021.100188

Manzocco, L., Valoppi, F., Calligaris, S., Andreatta, F., Spilimbergo, S., & Nicoli, M. C. (2017). Exploitation of κ-carrageenan aerogels as template for edible oleogel preparation. *Food Hydrocolloids*, *71*, 68–75. https://doi.org/https://doi.org/10.1016/j.foodhyd.2017.04.021

Nazarov, R., Jin, H. J., & Kaplan, D. L. (2004). Porous 3-D scaffolds from regenerated silk

fibroin. *Biomacromolecules*, *5*, 718–726. https://doi.org/10.1021/bm034327e

Nguyen, B. T., Balakrishnan, G., Jacquette, B., Nicolai, T., Chassenieux, C., Schmitt, C., & Bovetto, L. (2016). Inhibition and promotion of heat-induced gelation of whey proteins in the presence of calcium by addition of sodium caseinate. *Biomacromolecules*, *17*, 3800–3807. https://doi.org/10.1021/acs.biomac.6b01322

Nicolai, T. (2016). Formation and functionality of self-assembled whey protein microgels. *Colloids and Surfaces B: Biointerfaces*, *137*, 32–38. https://doi.org/10.1016/j.colsurfb.2015.05.055

Nicolai, T., & Durand, D. (2013). Controlled food protein aggregation for new functionality. *Current Opinion in Colloid and Interface Science*, *18*, 249–256. https://doi.org/10.1016/j.cocis.2013.03.001

Plazzotta, S., Calligaris, S., & Manzocco, L. (2020). Structural characterization of oleogels from whey protein aerogel particles. *Food Research International*, *132*, 109099. https://doi.org/10.1016/j.foodres.2020.109099

Rodríguez-Dorado, R., López-Iglesias, C., García-González, C. A., Auriemma, G., Aquino, R. P., & Del Gaudio, P. (2019). Design of aerogels, cryogels and xerogels of alginate: Effect of molecular weight, gelation conditions and drying method on particles' micromeritics. *Molecules*, *24*. https://doi.org/10.3390/molecules24061049

Selmer, I., Karnetzke, J., Kleemann, C., Lehtonen, M., Mikkonen, K. S., Kulozik, U., & Smirnova, I. (2019). Encapsulation of fish oil in protein aerogel micro-particles. *Journal of Food Engineering*, *260*, 1–11. https://doi.org/10.1016/j.jfoodeng.2019.04.016

Selmer, I., Kleemann, C., Kulozik, U., Heinrich, S., & Smirnova, I. (2015). Development of egg white protein aerogels as new matrix material for microencapsulation in food. *The Journal of Supercritical Fluids*, *106*, 42–49. https://doi.org/https://doi.org/10.1016/j.supflu.2015.05.023

Sharma, V., Shahnaz, T., Subbiah, S., & Narayanasamy, S. (2020). New insights into the remediation of water pollutants using nanobentonite incorporated nanocellulose chitosan based aerogel. *Journal of Polymers and the Environment*, *28*, 2008–2019. https://doi.org/10.1007/s10924-020-01740-9

Shimada, K., & Cheftel, J. C. (1988). Texture characteristics, protein solubility, and sulfhydryl group/disulfide bond contents of heat-induced gels of whey protein isolate. *Journal of Agricultural and Food Chemistry*, *36*, 1018–1025. https://doi.org/10.1021/jf00083a029

Subrahmanyam, R., Gurikov, P., Dieringer, P., Sun, M., & Smirnova, I. (2015). On the road to biopolymer aerogels-Dealing with the solvent. *Gels*, *1*, 291–313.

https://doi.org/10.3390/gels1020291

www.cost-aerogels.eu. AERoGELS COST Action. Retrieved May 2, 2021, from https://cost-aerogels.eu/

Zhang, H., Li, Y., Xu, Y., Lu, Z., Chen, L., Huang, L., & Fan, M. (2016). Versatile fabrication of a superhydrophobic and ultralight cellulose-based aerogel for oil spillage clean-up. *Physical Chemistry Chemical Physics*, *18*, 28297–28306. https://doi.org/10.1039/c6cp04932j

Figure captions

Figure 1. Visual appearance and SEM images of whey protein aerogels obtained by freeze-drying (FD) and supercritical CO_2-drying (SCD). FD: A) Visual appearance; SEM images at 1000 x and 30 kV (B) and 25000 x and 30 kV (C); SCD: D) Visual appearance; SEM images at 1000 x and 10 kV (E) and 25000 x and 20 kV (F). Size bar in images B) & E): 100 µm; C) & F): 5 µm.

Figure 2. Moisture adsorption as a function of a_w of whey protein aerogels obtained by freeze-drying (FD) and supercritical CO_2-drying (SCD). Symbols: experimental data; Lines: estimated by the Freundlich model.

Figure 3. Glass transition temperature of whey protein aerogels obtained by freeze-drying (FD) and supercritical-CO_2-drying (SCD) as a function of weight fraction. Symbols: experimental data; Lines: estimated by Gordon-Taylor equation.

Figure 4. Water (A) and oil (B) absorbed by whey protein aerogels obtained by freeze-drying (FD) and supercritical-CO_2-drying (SCD) as a function of time. The visual appearance of the aerogels upon absorption is also shown.

Colour is not required for any figures in print.

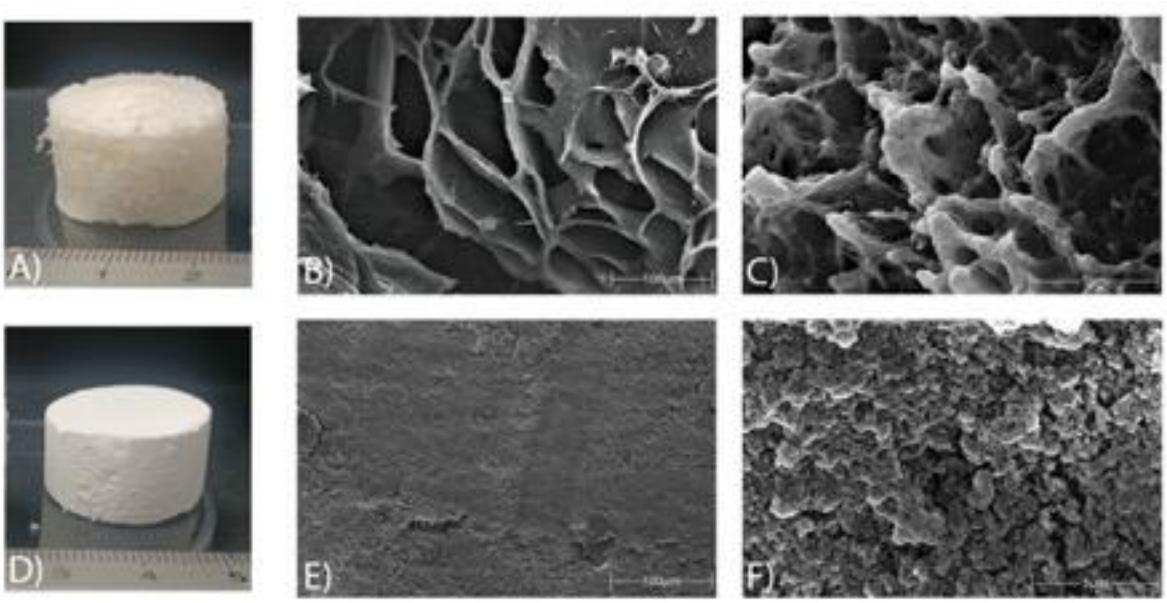

Figure 1. Visual appearance and SEM images of whey protein aerogels obtained by freeze-drying (FD) and supercritical CO_2-drying (SCD). FD: A) Visual appearance; SEM images at 1000 x and 30 kV (B) and 25000 x and 30 kV (C); SCD: D) Visual appearance; SEM images at 1000 x and 10 kV (E) and 25000 x and 20 kV (F). Size bar in images B) & E): 100 µm; C) & F): 5 µm.

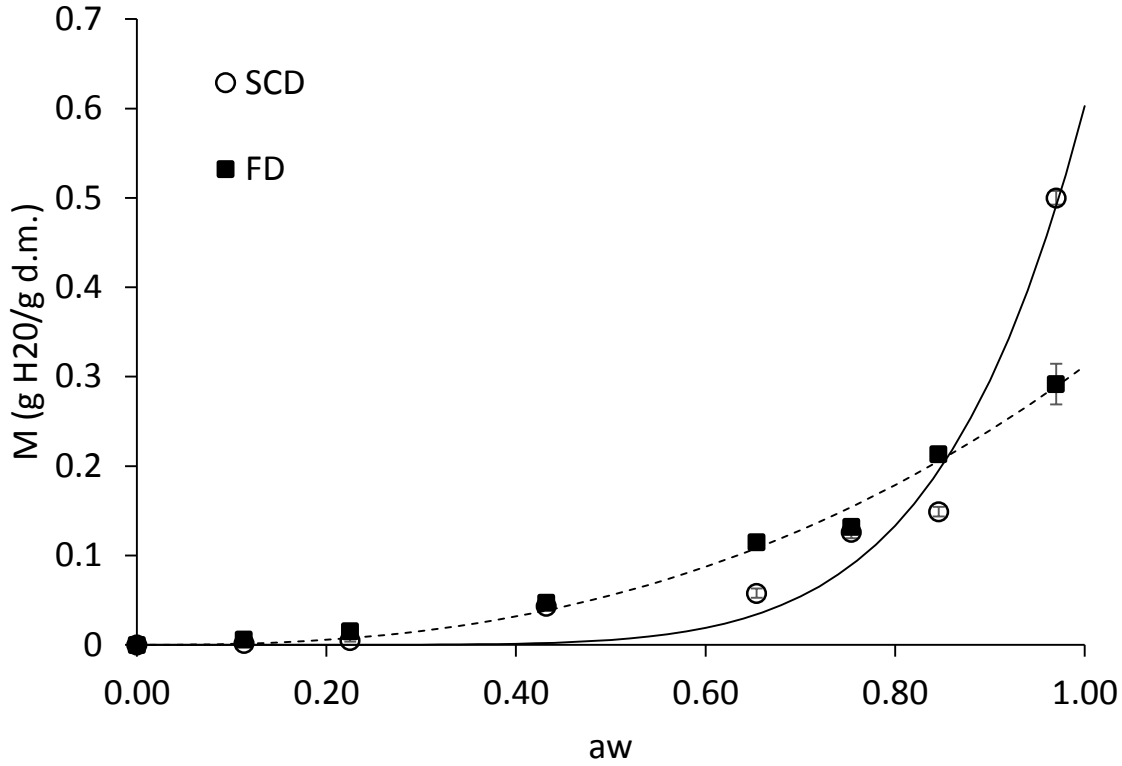

Figure 2. Moisture adsorption as a function of a_w of whey protein aerogels obtained by freeze-drying (FD) and supercritical CO_2-drying (SCD). Symbols: experimental data; Lines: estimated by Freundlich model.

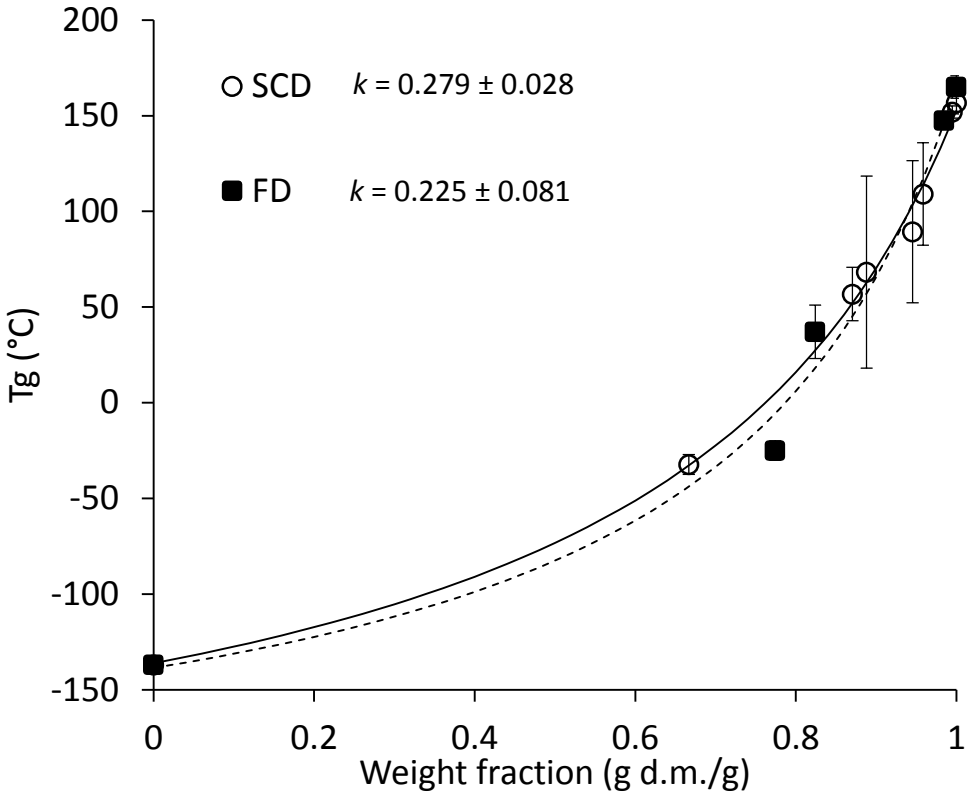

Figure 3. Glass transition temperature of whey protein aerogels obtained by freeze-drying (FD) and supercritical-CO_2-drying (SCD) as a function of weight fraction. Symbols: experimental data; Lines: estimated by Gordon-Taylor equation.

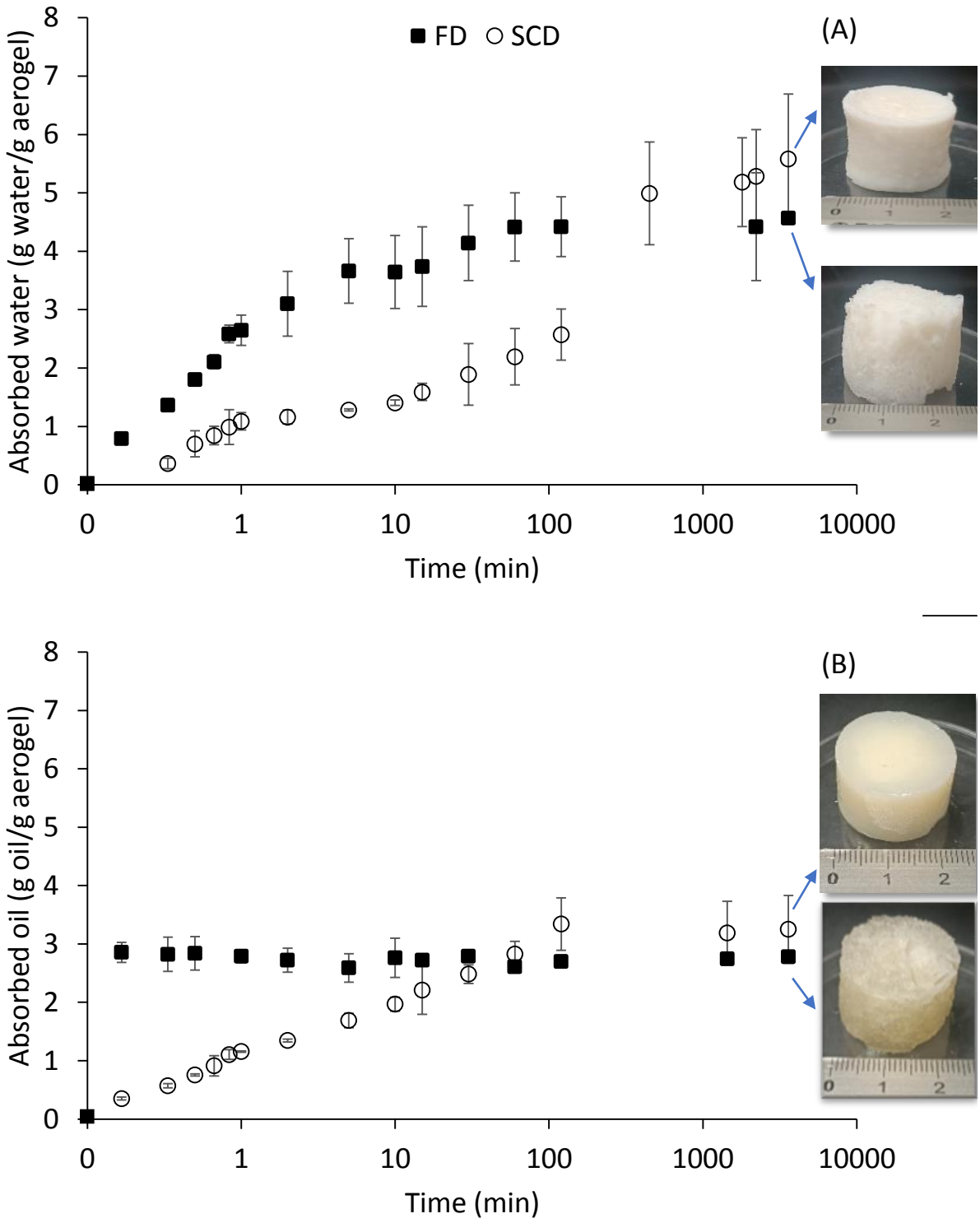

Figure 4. Water (A) and oil (B) absorbed by whey protein aerogels obtained by freeze-drying (FD, filled squares) and supercritical-CO_2-drying (SCD, open circles) as a function of time. The visual appearance of the aerogels upon absorption is also shown.

Conflict of Interest and Authorship Conformation Form

The Authors declare that:

- ✓ All authors have participated in (a) conception and design, or analysis and interpretation of the data; (b) drafting the article or revising it critically for important intellectual content; and (c) approval of the final version.

- ✓ This manuscript has not been submitted to, nor is under review at, another journal or other publishing venue.

- ✓ The authors have no affiliation with any organization with a direct or indirect financial interest in the subject matter discussed in the manuscript

CRediT authorship contribution statement

S.C. and L.M. conceived the original idea; S.P. and L.M. planned the experiments, S.P. carried out the experiments and performed data analysis; L.M. wrote the manuscript draft with support from other authors. J.P, A.d.V. and D.R. performed microscopic analyses and revised the manuscript. All the authors revised the final manuscript. S.C. and L.M. supervised the project.